Dual Band Planar Microwave Sensor for Dielectric Characterization using Solid and Liquid Sample

Norhanani Abd Rahman[1,3], Zahriladha Zakaria[1] , Rosemizi Abd Rahim[2], Yosza Dasril[1], Amyrul Azuan Mohd Bahar[1]

[1]*Centre for Telecommunication Research & Innovation, Faculty of Electronics and Computer Engineering, Universiti Teknikal Malaysia Melaka (UTeM), 76100 Durian Tunggal, Melaka, Malaysia.*

[2]*School of Computer and Communication Engineering, University Malaysia Perlis (UniMAP), Perlis, Malaysia.*

[3]*Department of Electrical Engineering, Polytechnics Seberang Perai (PSP), Pulau Pinang, Malaysia.*

norhanani80@gmail.com

***Abstract*—Dual band Complementary Folded Arm (CFA) split ring resonator is designed to determine the dielectric properties of liquid and solid materials based on resonance frequency shifting. The structure resonator is light, small and low-cost and it operates at two resonant frequencies simulated by ANSYS HFSS-15 software. The advantages of this sensor are to identify the dielectric properties of two different samples for a solid sample at 2.5GHz and several common liquids at 3.9GHz. The results show the good performance of the shift of resonance frequency at the different dielectric values and achieve the high-quality factor compared with other RF sensors with 446 and 506 respectively. Due to this, the resonator can be a highly credible sensor for bio-sensing and food quality industry.**

***Index Terms*—Dual Mode, DMS, DGS, Q-factor, Solid, Liquid**

I. INTRODUCTION

Nowadays, industrial development that is rapidly growing at this time requires accurate measurement of the characterization of the material that meets the criteria - cost-effective, highly accurate, compact, and it is mainly used to assess the quality and to identify characteristics of the material in the food industry, agriculture [1] and bio-sensing [2]. Many techniques have been designed appropriately for the specific material based on a set of frequencies, non-resonator or resonator methods [3] to determine the dielectric constant of the complex permittivity.

The non-resonant methods, over the frequency range, can be used to determine the electromagnetic properties [4], while this method gives a more accurate knowledge of dielectric properties over a limited frequency range or a single frequency. The resonant methods such as the cavity perturbation technique accomplish the dielectric measurement with a higher degree of accuracy [5] and can provide better sensitivity as compared to the broadband methods. The preferred measurement technique is based on several factors such as frequency range, permeability and permittivity, homogeneous or isotropic, the form of material, sample size restrictions, destructive or nondestructive and cost. Based on the criteria, cavity waveguide perturbation [6], free-space transmission [7] open-ended coaxial probe[8], and planar transmission line technique [9] have been used for different applications for determining the material characterisation. In order to get a simple sample preparation, with the accuracy of resonant cavity methods in extracting local material properties, and to make it simply integrate with other microwaves, the planar transmission line is the best technique compared to other techniques. The advantages of using it lie in the ease of fabrication, compactness, low cost and easy handling [10]. The most commonly used is resonant methods because of their higher accuracy and sensitivity. In planar resonator methods, the MUT is placed either on the top of the resonator or inside the substrate depending on the maximum electric field location (E-Field). Therefore, the most structural planar microwave sensors for determining and detecting the dielectric properties in common solid or liquid to produce high-quality factor (Q-factor) [11], [12].

This paper presents the simulations of the sensor to produce stronger electric field concentration on a gap of Complementary Folded Arm (CFA) split ring resonator to obtain high Q-factor with two different resonant frequencies. The performance of the sensor also observes the shift of resonance frequency with a liquid sample using a capillary glass tube and an overlay sample placed over the resonator for the different widths, thickness and dielectric values. An analysis of the parameter will be helpful when it comes to designing the best resonator for the bio-sensing and food quality application.

II. DESIGN STRUCTURES

The most common structures of microstrip square open-loop resonator shown in Figure 1 frequently used in the filter, is now applied to the sensor design. The selected resonator structure (Figure 1(d)) works as a double tuned resonant circuit and will be gained in more compact configurations because of the halved number of resonators. Additionally, using dual mode can produce a design that has a compact size.

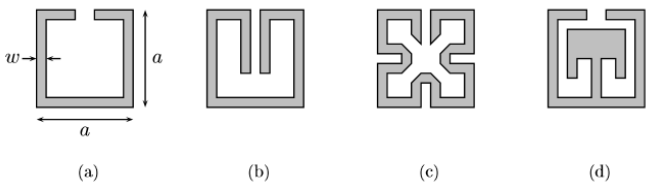

Figure 1: Square open loop resonator (SOLR) and some miniaturisation techniques. (a) Conventional SOLR. (b) Folded arms SOLR. (c) Meander line SOLR. (d) Dual mode SOLR [13]

The dual mode functions as two independent resonators that can provide a 50% reduction of the rectangular

resonator. There are two independent modes, and the coupling between the modes can be modified by the internal structure geometry [14]. Nevertheless, for the proposed sensor design, we choose to use the closed loop resonator to eliminate two independent modes to a single mode based on the operating resonant frequency of the resonator.

This dual mode square close loop resonator loaded rectangular patch with (LxW), and the length, l of the folded arm that determines the resonance frequency as illustrated in Figure 2(a) is designed on the etched coupled defected microstrip structure (DMS) on the patch resonators as shown in figure 2(b). It has the advantage of narrow band performance. The length of the resonator is half wavelength, and it correlated with the resonant frequency, f_c using the Equation (1) [15].

$$l = \frac{c}{2\sqrt{\varepsilon_{eff}}} x \frac{1}{f_c} \tag{1}$$

where, ε_{eff} is the effective permittivity of the materials in the sensor and c, is the velocity of light derived in Equation (2).

$$\varepsilon_{eff} = \frac{\varepsilon_r + 1}{2} + \frac{\varepsilon_r - 1}{2}\left[\frac{1}{\sqrt{1+12(h/w)}}\right] \text{For} \quad h/w \geq 1 \tag{2}$$

The frequency of resonance can be known prior to the compatible folded arm loading by the length and width of the patch. Despite that, the length l is the parameter that regulates the resonant frequency of our proposed sensor.

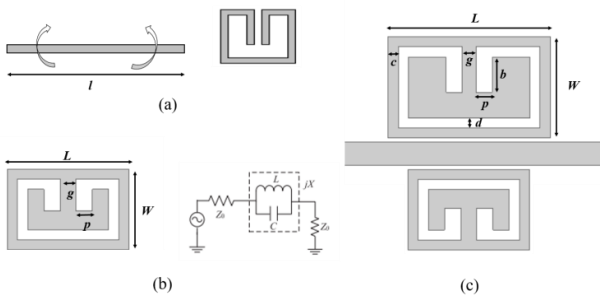

Figure 2: (a) The folded arm resonator can be obtained by folding a straight open resonator (b) CFA structure and an equivalent circuit (c) Dual Band CFA

Each single mode resonator is the same as the combined LC circuit. It produces a pole (transmission zero) on the frequency of the resonance. To increase the narrow band single mode resonator needs to be connected in a cascade structure to dual mode. The 'p' and 'g' parameters which represent the capacitance and inductance are between the folded arms in the middle of the resonator. Placing the optimised CFA resonator at the top and bottom of the 2.3mm width feedline in a different electrical length is demonstrated in Figure 2(c) and Table 1. Two independently controllable resonance frequencies with 44mm length for 2.5GHz and 29mm length for 3.8GHz based on centre length of complementary folded arm structure can be gained.

Table 1
Parameters of Dual Band CFA

Frequency	Parameters	W_r	L_r	g	p	d	c	b
2.5GHz	Value (mm)	10	16	1.42	1.56	1	1	3.5
3.8GHz		8	12	1.6	1.6	1	1	2.17

III. Result And Discussion

A. Resonator Analysis

The design of this CFA sensor is based on the bandstop circuits to perform multichannel sensing with different sizes and placed opposite each other along the feed line [16]. Hence, the sensor indicates various resonances with each representing a single channel that is controlled by an individual resonator. Since every resonator has a high-Q resonance at a unique frequency, the mutual interaction among the resonators is minimal. Therefore, each resonance is responsive to the existence of a sample placed over the resonator.

Higher Q-factor achievement is needed for this resonator to be more sensitive. Therefore, the single geometrical slots embedded on the ground plane namely a defected ground structure (DGS) to produce a high-performance component in microstrip circuits [17]. The development of patterned DGS also focuses on obtaining the narrow band on the high Q-factor by using the conventional methods that were based on some trial and error iterative methods [18].

For the purpose sensor, the output of analysis resonator with DGS structure as shown in Figure 3(a) and Figure 3(b) was simulated by HFSS 15.0 software on Rogers 5880 with a substrate of the relative dielectric constant of 2.2 and thickness 0.787mm. The selection of a thin copper thickness 0.0175mm and a small value of loss tangent 0.0009 seek to increase the sensitivity to the material. The DGS structures are parallel with the square size of dual mode on the top, and the parameters are summarised in Table 2.

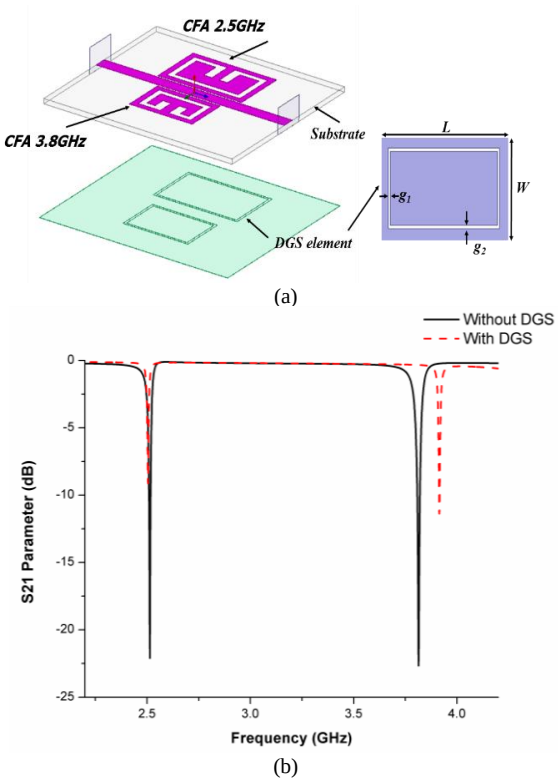

Figure 3: (a)Dual Band CFA with DGS structure, (b) S21 Parameter between sensor without DGS and DGS

Table 2
Parameters of DGS Structure

Frequency	Parameters	L	W	g_1	g_2
2.5GHz	Value (mm)	16	10	0.3	0.2
3.8GHz		12.4	12.4	0.4	0.4

The length and width of the resonator structure will determine the resonant frequency before loading the CFA sensor. However, after introducing DGS, there has been a slight shift of the resonant frequency from 3.8GHz to 3.9GHz, but the value of Q-factor increases, and the insertion loss decreases as compiled in Table 3. The calculation of the unloaded Q-factor can be derived from Equation (3), and Figure 4 illustrates the measurement of Q-factor based on the resonant frequency, f_0 and the frequency bandwidth, Δf of the resonant peak at -3dB power points [19].

$$Q = \frac{2 f_0}{\Delta f} \tag{3}$$

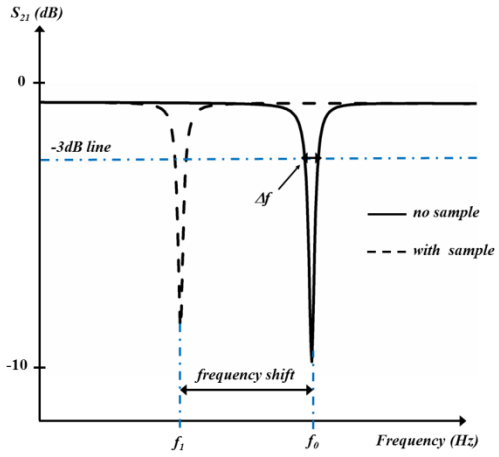

Figure 4:. Measurement of unloaded quality factor and frequency shift with a loading sample.

Table 3
Simulation result of CFA sensor without DGS and DGS

Parameter	Without DGS		With DGS	
Frequency (GHz)	2.5	3.8	2.5	3.9
S21 (dB)	-22.0964	-22.6618	-9.1443	-11.3847
Q Factor	201	181	446	506

B. Experimental Studies

Dielectric properties of materials or permittivity are affected by many factors, including frequency, moisture content and temperature. Dielectric properties that can vary significantly with frequency based on the permittivity spectrum has to be measured with high sensitivity over a broad frequency range from 1 kHz to 10 GHz [20]. Therefore, the characteristics of the resonant frequency selection for the sensor depend on the application besides the structured approach (topology, material and size). For the purposed sensor, the operation on S-band took place in most of the microwave applications, and it was compatible with lab-on-a-chip. Hence, it will meet the needs of high sensitivity devices with minimal cost for food and bio-sensing applications. The first resonant frequencies in the sensor 3.9GHz targeting at the microfluidic applied in biosensing applications are implemented to improve the reliability of the proposed sensor. The sensor operating at a higher frequency because of its capability to bypass the cell plasma membrane to penetrate into, and react directly with, the intracellular content especially its water concentration in MUT [21]. Thus, the second resonant frequency 2.5GHz is extensively being used in industrial, scientific and medical (ISM) frequency bands [22] focusing on the food industry for solid MUT because the dielectric properties of materials are highly correlated with the amount of water in MUT. The dielectric properties are also highly variable with the frequency of the alternating fields applied to them [1].

C. Microfluid Channel Design and Analysis of Liquid Sample.

A channel for micro-capillary loading is made on one of the resonators. To decide upon the location of a capillary slot, the magnitude of the electric field distribution of the dual mode loaded on a patch is plotted in Figure 5(a), (b). The important part is to know the area of the highest sensitivity of the dual mode slot so that full benefits of the resonance originating from the capillary slot on the sensor can be retained.

Referring to [23], we use the capillary glass tube for the microfluidic channel with a dielectric constant of 5.5. The inner and outer radii of the capillary glass are 0.745mm and 0.85mm, respectively. Figure 5 (c), (d) demonstrated the capillary slot position and the electromagnetic fields around the capillary glass tube.

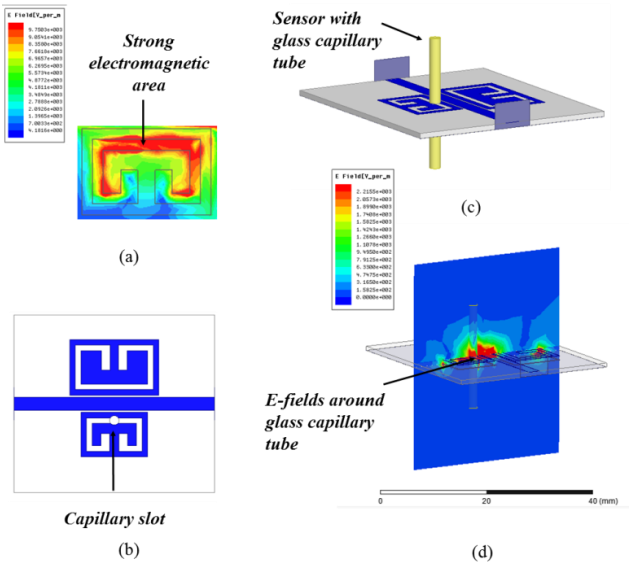

Figure 5: (a) Location of a capillary slot (b) The magnitude of the electric field distribution (c) Capillary slot position, (d) Electromagnetic fields around the capillary glass tube

Several common solvents with different dielectric constant were chosen to load into the capillary glass tube to see changes in resonant frequency based on the perturbation of the electric field. This is because the frequency of resonance dual mode resonator is dependent on the permittivity of its surrounding materials. However, to obtain the best performance, the maximum frequency shift will occur while filling the minimum fluid volumes [24]. The empty capillary glass tube is used as a reference model because of its known permittivity and loss tangent of air. The S-parameter simulation after loading some liquids is described in Figure 6 to indicate the sensitivity of the sensor.

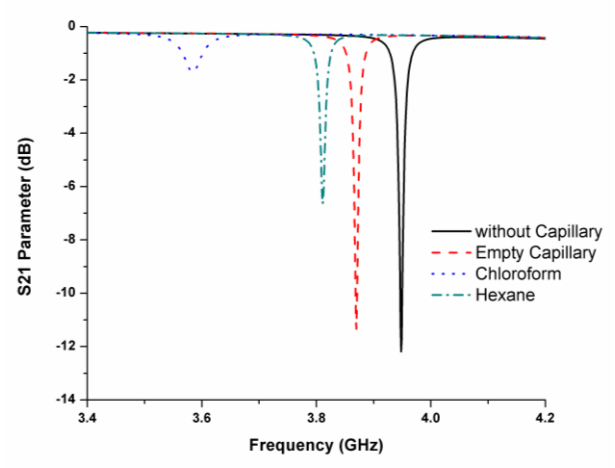

Figure 6: Resonant frequency values with different dielectric samples of liquid.

The frequency response of the simulation results with the presence of several common solvents for 3.9GHz dual mode sensor is shown in Table 4. To investigate the shifts and flux losses-based solvent properties, several Chloroform and Hexane solvents with standard concentration have been simulated. Once the capillary is secured into the hole regions, the capacitance of the structure is affected by the solvent, which in turn generates an interference resonator.

Table 4
Frequency Shift with Different Dielectric Samples

Parameter	Empty Capillary	Chloroform	Hexane
Relative Permittivity (ε_r)	5.5	4.81	1.88
Frequency (GHz)	3.87	3.58	2.56
Frequency Shift (MHz)	30	320	1340

D. Analysis of Solid Sample.

Based on research [25], the size and thickness of the overlay dielectric material sample will affect the permittivity. More than 9% of the substrate height for the sample thickness and sample size must be greater than 18.3% of the guided wavelength (λ_g). This situation can be illustrated in Figure 7 shows that the wave propagates stronger in the line enclosed into minimal thickness and size of the overlay sample and substrate. However, if the sample thickness has increased or enlarged, the excess of the value of the experiment, the fringing fields will weaken. This effect will not interfere with permittivity.

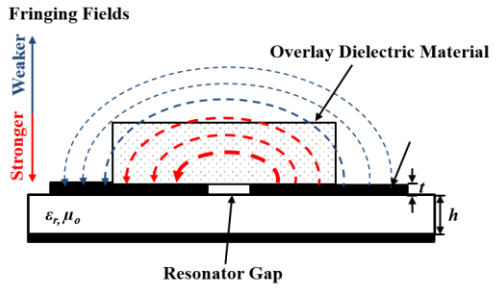

Figure 7: Interaction of electric fields with overlay dielectric material.

The unknown dielectric samples should have at least one flat surface of area greater than, or equal to, the area of the sensor structure so that they come in close contact with the full area of the resonator surface without any air gap [26]. In this work, the analysis for solid samples size was carried out by an overlay is known sample 0. 787mm thickness placed over another dual mode resonator as demonstrated in Figure 8. The dimension of the sample started with 20mm x 14mm (length x width), and the range of the size selected in different lengths and widths overlay the samples to determine the behaviour of the resonant frequencies. The selected sample size should not touch the feed line as it will affect the resonant frequency of another resonator.

The simulation result is presented in Figure 9(a) revealing that the size of the overlay sample is increased and the resonance frequencies will be reduced. The smaller size of the overlay sample produced 8% frequency shift, while the size becomes a constant starting from the size of 20x14 mm which yielded 5.6% of frequency shift. This happens due to the higher rate of perturbation when the overlay sample size is increased, and more fringing fields have based it more on the overlay sample. Meanwhile, in the sample thickness analysis, the range of thickness is from 0.787mm to 8.567mm, which is more than 9% of the substrate which shows that the thickness of the overlay sample increases, as illustrated by Figure 9(b). Minimum frequency shift in the thin thickness is noted to be 5.6%, and the maximum shift was 9.2% for the height thickness, as the maximum fields are distressed by an overlay sample. The thickness height will lead to the maximum perturbation leading to a higher shift in the resonance frequency. Conversely, the low thickness of the overlay sample will bring about a small shift in the resonance frequency.

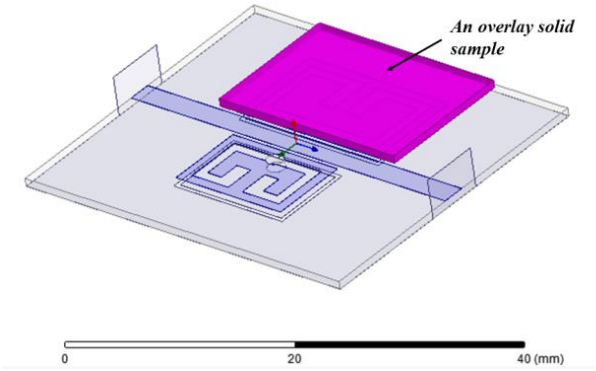

Figure 8: An overlay solid sample test

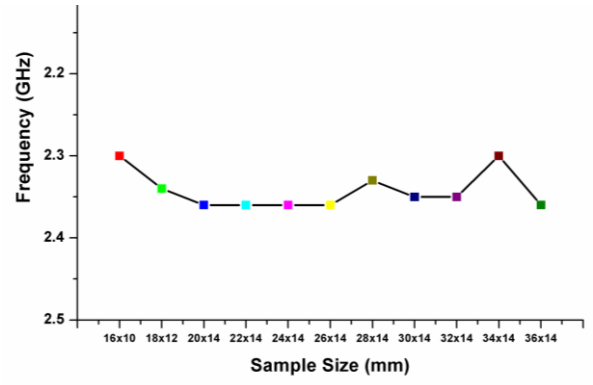

(a)

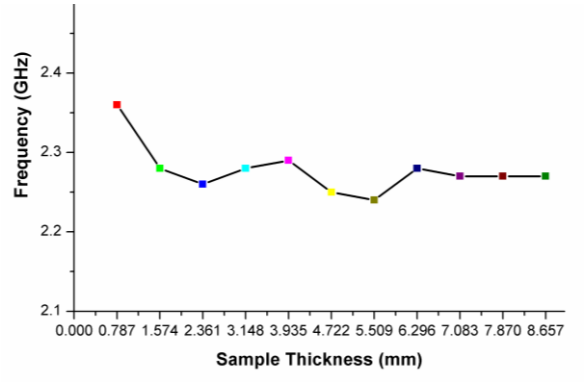

(b)

Figure 9: Relation between the frequency with sample size and thickness

The proposed study on different sample sizes seeks to obtain high-sensitivity sensors in space to achieve a high Q factor. An overlay sample is needed to place over the sensitive area of the sensor in a maximum electric field (E-field) region [27]. Three different types of the sample with various dielectric properties used Roger 5880, Roger 4350 and Teflon, to identify the ability of the design for various sensing applications. Each sample to be tested is placed over the dual mode resonator at the 2.5GHz resonant frequency.

Without the sample, the retrieve resonance frequency for the sample is 2.5GHz, upon loading; the resonance frequency is shifted down following the higher value of the dielectric constant of samples. Results can be acquired and compared in Figure 10 and summarised in Table 5. As shown in the graph, the resonance frequency changes to a lower frequency as the dielectric sample has a higher permittivity value.

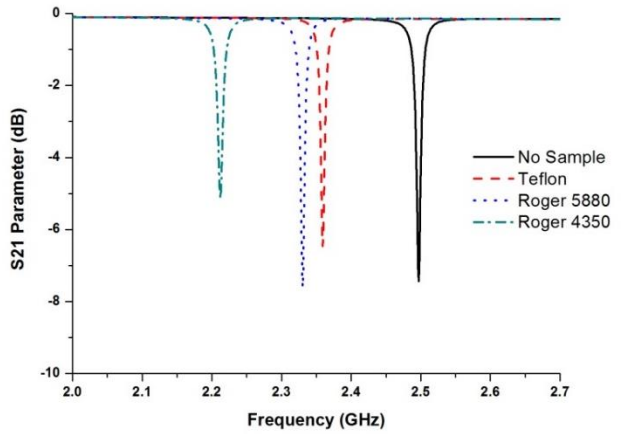

Figure 10. Resonant frequency values with a different dielectric with solid samples.

Table 5
Frequency Shift with Different Dielectric Samples.

Parameter	Teflon	Rogers 5880	Roger 4350
Relative Permittivity (ε_r)	2.1	2.2	3.48
Frequency (GHz)	2.36	2.33	2.21
Frequency Shift (MHz)	140	170	290

IV. Conclusions

A new dual band CFA sensor has been successfully designed and simulated. The structure of the sensor can detect the bio-sensing molecules with improved sensitivity by increasing the electric field distributions between the split structures. In addition, this purposed sensor will produce a high Q-factor for 2.5GHz and 3.9GHz resonator with 446 and 506 respectively and determine the dielectric properties of liquid and solid samples. Every single material has different permittivity value. The shifting of frequency reflects the properties of the material itself. In other words, the permittivity can be extracted from the frequency shifting response. Therefore, one can reliably measure the quality and safety of the materials based on this valuable parameter (permittivity) which is intensively applied in bio-sensing and food industry applications. The performance of resonator is determined by measuring permittivity of a dielectric sample in terms of the shift in resonant, and the result shows good achievement with different dielectric values. The comparison of the quality factor of the proposed sensor with the other RF sensors in the electrical characteristics (stopband frequency) is summarised in Table 6. It is notable that the proposed sensor for the determination of material characterisation shows higher sensitivity with high Q factor. This resonator will contribute to bio-sensing and food quality applications in future that need devices that are more sensitive with high Q-factor, low-cost and compactness. The future work can be done by verifying and comparing between simulation results through experimental works.

Table 6
Comparison of Proposed Sensor and RF Sensor Regarding Quality Factor and Resonant Frequency.

References	Sensing Material	Frequency	Q factor
[28]	Semi-solid	180MHz	80
[29]	Solid	2.65GHz	80
[30]	Liquid	5GHz	174
[19]	Solid	5GHz	250
Proposed Sensor	Solid Liquid	2.5GHz 3.9GHz	446 506

Acknowledgement

The author gratefully acknowledges the Centre for Research & Innovation Management (CRIM) UTeM and Universiti Teknikal Malaysia Melaka (UTeM), also the Ministry of Higher Education (MOHE), Malaysia for funding this work under FRGS/1/2015/SG02/FKEKK/03/F00265. This study was undertaken during the study leave of the main author under the 2016 Federal Training (HLP) scholarship scheme awarded by MOHE.

References

[1] S. Trabelsi and S. O. Nelson, "Microwave Sensing of Quality Food Products," *IEEE Instrum. Meas. Mag.*, vol. 19, no. 1, pp. 36–41, 2016.

[2] A. Rydosz, E. Brzozowska, S. Gorska, K. Wincza, A. Gamian, and S. Gruszczynski, "A Broadband Capacitive Sensing Method for Label-Free Bacterial LPS Detection," *Biosens. Bioelectron.*, vol. 75, pp. 328–336, 2016.

[3] A. A. Rammah, Z. Zakaria, E. Ruslan, and A. A. M. Isa, "Comparative Study of Materials Characterization using Microwave Resonators," *Aust. J. Basic Appl. Sci.*, vol. 9, no. 1, pp. 76–85, 2015.

[4] P. M. Narayanan, "Microstrip transmission line method for broadband permittivity measurement of dielectric substrates," *IEEE Trans. Microw. Theory Tech.*, vol. 62, no. 11, pp. 2784–2790, 2014.

[5] A. K. Jha, S. Member, M. J. Akhtar, and S. Member, "A Generalized Rectangular Cavity Approach for Determination of Complex Permittivity of Materials," *IEEE Trans. Instrum. Meas.*, pp. 1–10, 2014.

[6] A. Foudazi and K. M. Donnell, "Effect of Sample Preparation on Microwave Material Characterization by Loaded Waveguide Technique," *IEEE Trans. Instrum. Meas.*, vol. 65, no. 7, pp. 1669–1677, 2016.

[7] P. Skocik and P. Neumann, "Measurement of Complex Permittivity in

Free Space," *Procedia Eng.*, vol. 100, no. 4, pp. 100–104, 2015.
[8] T. Reinecke, L. Hagemeier, S. Ahrens, M. Klintschar, and S. Zimmermann, "Permittivity Measurements for the Quantification of Edema in Human Brain Tissue – Open-ended coaxial and coplanar probes for fast tissue scanning," *2014 IEEE Sensors*, pp. 681–683, 2014.
[9] C. Sen Lee and C. L. Yang, "Thickness and permittivity measurement in multi-layered dielectric structures using complementary split-ring resonators," *IEEE Sens. J.*, vol. 14, no. 3, pp. 695–700, 2014.
[10] M. S. Boybay and O. M. Ramahi, "Material characterization using complementary split-ring resonators," *IEEE Trans. Instrum. Meas.*, vol. 61, no. 11, pp. 3039–3046, 2012.
[11] A. A. Abduljabar, D. J. Rowe, A. Porch, and D. A. Barrow, "Novel Microwave Microfluidic Sensor Using a Microstrip Split-Ring Resonator," *IEEE Trans. Microw. Theory Tech.*, vol. 62, no. 3, pp. 679–688, 2014.
[12] N. A. Rahman, Z. Zakaria, R. A. Rahim, and Y. Dasril, "Planar Microwave Sensors for Accurate Measurement of Material Characterization : A Review Refbacks," *TELKOMNIKA*, vol. 62, no. 274, p. 564604, 2017.
[13] L. M. Ledezma, "A Study on the Miniaturization of Microstrip Square Open Loop Resonators," 2011.
[14] A. V. V. Mannam and B. Y. R. Veeranki, "Design of Narrowband Band Pass Filter using Open-loop Square Resonators with Loading Element," *Indian J. Sci. Technol.*, vol. 9, no. December, pp. 1–9, 2016.
[15] M. H. Zarifi, S. Farsinezhad, K. Shankar, M. Daneshmand, and S. Member, "Liquid Sensing Using Active Feedback Assisted Planar Microwave Resonator," *IEEE Microw. Wirel. Components Lett.*, vol. 25, no. 9, pp. 621–623, 2015.
[16] W. Withayachumnankul, K. Jaruwongrungsee, A. Tuantranont, C. Fumeaux, and D. Abbott, "Metamaterial-based microfluidic sensor for dielectric characterization," *Sensors Actuators, A Phys.*, vol. 189, pp. 233–237, 2013.
[17] M. T. Khan, M. A. Zakariya, M. N. M. Saad, Z. Baharudin, and M. Z. U. Rehman, "Analysis and Realization of Defected Ground Structure (DGS) on Bandpass Filter," *5th Int. Conf. Intell. Adv. Syst.*, pp. 1–4, 2014.
[18] M. K. Khandelwal, B. K. Kanaujia, and S. Kumar, "Defected Ground Structure : Fundamentals, Analysis, and Applications in Modern Wireless Trends," *Hindawi Int. J. Antennas Propag.*, vol. 2017, 2017.
[19] I. M. at Rusni, A. Ismail, A. R. eda H. Alhawari, M. N. izar Hamidon, and N. A. zah Yusof, "An Aligned-Gap and Centered-Gap Rectangular Multiple Split Ring Resonator for dielectric sensing applications," *Sensors (Basel).*, vol. 14, no. 7, pp. 13134–13148, 2014.
[20] S. Kulkarni and M. S. Joshi, "Design and Analysis of Shielded Vertically Stacked Ring Resonator as Complex Permittivity Sensor for Petroleum Oils," *IEEE Trans. Microw. Theory Tech.*, vol. 63, no. 8, pp. 2411–2417, 2015.
[21] C. Dalmay, J. Leroy, A. Pothier, and P. Blondy, "Development of high frequency microfluidic biosensors for intracellular analysis," *Procedia Eng.*, vol. 87, no. i, pp. 54–57, 2014.
[22] M. A. H. Ansari, "Dual Band Microwave Sensor for Dielectric Characterization of Dispersive Materials," *Asia-Pacific Microw. Conf.*, vol. 1, pp. 1–3, 2015.
[23] A. A. Mohd Bahar and Z. Zakaria, "Dielectric Analysis of Liquid Solvents Using Microwave Resonator Sensor for High Efficiency Measurement," *Microw. Opt. Technol. Lett.*, vol. 54, no. 12, pp. 2781–2784, 2017.
[24] A. Salim and S. Lim, "Complementary Split-Ring Resonator-Loaded Microfluidic Ethanol Chemical Sensor," *Sensors (Switzerland)*, vol. 16, no. 11, 2016.
[25] M. T. Jilani, W. P. Wen, L. Y. Cheong, and M. Z. U. K. Rehman, "Determination of Size- Independent Effective Permittivity of An Overlay Material Using Microstrip Ring Resonator," *Microw. Opt. Technol. Lett. /*, vol. Vol. 58, N, pp. 4–9, 2016.
[26] S. P. Chakyar, S. K. Simon, C. Bindu, J. Andrews, and V. P. Joseph, "Complex permittivity measurement using metamaterial split ring resonators," *J. Appl. Phys.*, vol. 121, no. 5, 2017.
[27] D. Pozar, *Microwave Engineering Fourth Edition*. John Wiley & Sons Ltd, 2005.
[28] H. J. Lee *et al.*, "A planar split-ring resonator-based microwave biosensor for label-free detection of biomolecules," *Sensors Actuators, B Chem.*, vol. 169, pp. 26–31, 2012.
[29] M. A. H. Ansari, A. K. Jha, and M. J. Akhtar, "Design and Application of the CSRR-Based Planar Sensor for Noninvasive Measurement of Complex Permittivity," *IEEE Sens. J.*, vol. 15, no. 12, pp. 7181–7189, 2015.
[30] I. M. Rusni, A. Ismail, A. R. Alhawary, M. N. Hamidon, and N. A. Yusof, "Aligned-Gap Multiple Split Ring Resonator for Dielectric Sensing Application," *Int. Conf. Eng. Technol. Technopreneush.*, pp. 143–147, 2014.